Journal of Mines, Metals and Fuels, *71(10): 1601-1611; 2023. DOI: 10.18311/jmmf/2023/35806*

Print ISSN : 0022-2755

Journal of Mines, Metals and Fuels

Contents available at: *www.informaticsjournals.com/index.php/jmmf*

CFD Analysis of Pulsatile Non-Newtonian Blood Flow in a Multi-Staged Stenosed Bifurcated Carotid Artery

Monica Anand[1*], Seema Aggarwal[2], Harshit Raj[3], Diksha Arora[3] and Dhruv Gajjar[3]

[1]Department of Mathematics, Ramaiah Institute of Technology, Bangalore – 560054, Karnataka, India; amonica@msrit.edu

[2]Department of Physics, Ramaiah Institute of Technology, Bangalore – 560054, Karnataka, India; smabgl.11@gmail.com

[3]Department of Mechanical Engineering, Ramaiah Institute of Technology, Bangalore – 560054, Karnataka, India; hraj1222@gmail.com; dikshaarora68@gmail.com; gajjardhruv55@gmail.com

Abstract

Accumulation of plaque on the arterial walls leads to a cardiovascular condition known as Atherosclerosis. This leads to lumen stenosis, and when it occurs in the carotid artery, it can impede the blood-flow to the face, brain, and neck, potentially leading to a stroke. The aim of this paper is to provide a comprehensive study of the carotid artery under multiple stenosed conditions using Computational Fluid Dynamics. In this study, blood has been considered to be a non-Newtonian fluid exhibiting pulsatile flow based upon the Carreau model and a two-dimensional bifurcated human carotid artery has been modelled. The Navier-Stokes equations-based FVM (Finite Volume Method) is used to analyze the flow inside the artery, while RANS k-ω SST turbulence model has been applied in the analysis of parameters of blood under stenosed conditions. Four models based on different stages of stenosis (0%; 25%; 50% and 75%) have been developed with simulations run on Ansys to find the effects under stenosis. For all the simulations, 65:35 flow division has been used, indicating that 65% of the total blood flows through the Internal Carotid Artery and 35% flows through the External Carotid Artery. Velocity and pressure contour, velocity distribution on the modelled plane and wall shear stress on arterial walls are the primary parameters studied at varying timescales of a cardiac cycle. As the stenosis stage increases, the flow separation can be predicted with higher accuracy. With the help of these parameters, one can build and design better treatment choices, such as designing of stents with different materials or adding of Ag-Au (Silver - Gold) nanoparticles in the blood to change the hemodynamics.

Keywords: *Atherosclerosis, Computational Fluid Dynamics, Non-Newtonian Behaviour*

1.0 Introduction

In locations where flow is disrupted and wall shear stress is low, stenosis which is the narrowing of an artery lumen is likely to occur because of plaque formation and encroachment into the lumen. This causes more flow disturbances and increases wall shear stresses in stenoses which is more hemodynamically important. The flow becomes unstable in the post stenotic region as it slows down causing separation and recirculation of blood. For more severe constrictions, the blood flow becomes turbulent.

Additionally, the constriction may cause a dynamic pressure change on the artery's walls, causing the blood vessel to rupture and cause a stroke. The effect of chaotic flow on ensuing forces on and within the affected blood vessel epithelium and surrounding regions could be of major interest to us. There have been previous studies

**Author for correspondence*

done to examine the same using various numerical approaches and models.

Herschel-Bulkley, Bingham, along with "power-law fluids" model was used to model the non-Newtonian blood flow *via* stenosis. It was found that the disruptions, particularly in cases of stenosis that are severe, are worsened by the strength of the vortex formed and persisted beyond the geometrical obstruction[1]. Three axisymmetric and three symmetrical stenosed tubular models were used with varying degrees of stenosis stages to replicate pulsatile blood flow[2]. For every model, the focus was on the flow separation zone and the WSS distributions. The Newtonian model was compared with the Carreau and power law models that were used to simulate stenosis of 45% that had the characteristics of a trapezoidal profile. The results showed that the power law model has considerably smaller WSS and much more significant vortices than the Carreau model[3]. It was discovered that with the increase in stenosis height in moderate stenosis, the pressure drops, and the plug core radius and wall shear stress also increase[4]. The SST k-ω model was used to study the impact of turbulence transition on hemodynamic parameters during pulsatile flow through coronary arteries with various degrees of stenosis[5,6]. It was shown that the turbulence transition begins to occur at 50% stenosis and completely develops above 70% stenosis. It was also discovered that other hemodynamic factors for identifying plaques at risk of rupture include the existence of turbulence and the location of the transition from a laminar to a turbulent state[5]. The relationship between high plaque risk and high wall shear stress was looked into using CFD. As per studies, high shear causes specific changes in endothelial cell behavior that intensify inflammation and accelerate the development of atherosclerotic lipid core[7]. The hemodynamic parameters were investigated using k-ω and k-ϵ models for patient specific elastic carotid artery using physiological pulses with high Oscillatory Shear Index (OSI) regions prone to stenosis. Results showed the formation of plaques in the regions with low rate of shear stress resulting in high sedimentation due to decreased velocity[8]. Computational study on various bifurcation angles were performed considering both Newtonian and Carreau-type non-Newtonian blood models. It was observed that the time-averaged wall shear stress was lower in the lowered-angled wall close to the bifurcation and greater away from it. Vorticity and helicity in fluid flow were produced as a result of the blending of various flow patterns over a cardiac cycle[9].

Based on the literature, the SST k-ω model is the best suited turbulent model for modelling flow under the condition of pulsatile flow. We choose the SST k-ω turbulence model to analyze the effect of different stages of stenosis in pulsatile blood flow based upon the Carreau non-Newtonian viscous model. Hemodynamic factors have been analyzed to study the severity due to multi-staged stenosis in terms of velocity, pressure and WSS. Important results were achieved from the current study, highlighting the behavior of blood under stenosed condition and identifying atherosclerosis at an earlier stage of the illness.

2.0 Analysis and Modelling

2.1 Governing Equations

The governing equations provide the mathematical formulations of the laws of conservation in physics, and they have been used to design a solution based on the flow characteristics and existing boundary conditions. The following variant of the Navier-Stokes equation meets the continuity and momentum equations requirements for two-dimensional, unstable, incompressible and laminar flow

$$\nabla \cdot \vec{u} = 0 \tag{1}$$

$$\rho\left(\frac{\partial \vec{u}}{\partial t} + \vec{u}.\nabla\right) = -\nabla p + \mu \nabla^2 \vec{u} \tag{2}$$

Where, $\vec{u}$ represents velocity, p pressure under static conditions, ρ fluid density, and μ dynamic viscosity. When laminar flows are present, these parameters are used. For turbulent flows, the following changes are made to the momentum equation[10]:

$$\frac{\partial \rho u_i}{\partial t} + \frac{\partial}{\partial x_j}\left(\rho\overline{u_i u_j} + \rho\overline{u'_i u'_j}\right) = -\frac{\partial \bar{p}}{\partial x_i} + \frac{\partial \overline{\tau}_{ij}}{\partial x_j} \tag{3}$$

Where, $\bar{u}_i$ and $\bar{u}_j$ represent velocity components in x_i and x_j direction, $\rho u'_i u'_j$ represent Reynolds stresses, p represents pressure and τ_{ij} is the mean viscous stress tensor.

2.2 Blood Flow Model

Blood is a non-Newtonian fluid that is viscous and incompressible with a constant density of 1060 kg/m^3. The Carreau viscosity model, which is regarded to be the most suited for such simulations and also accounts for the shear-thinning behavior of blood, is used to simulate the intricate rheological behavior of blood in pulsatile non-Newtonian blood flow simulations[10]. The viscosity model (μ) is given as:

$$\mu = \mu_\infty + (\mu_0 - \mu_\infty)\left[1 + \lambda\dot{\gamma}^2\right]^{\frac{n-1}{2}} \quad (4)$$

Where, $\mu_\infty = 0.00345\ Pa.s$ is the infinite shear viscosity, $\mu_0 = 0.0560\ Pa.s$ is the blood viscosity at zero shear rate, $\dot{\gamma}$ is the instantaneous shear rate, $\lambda = 3.313\ s$ is the time constant, $n = 0.3568$ is the power-law index.

2.3 Turbulence Model

The k-ω SST is a hybrid model that, by intelligently switching between the two and combines the benefits of the k-ω and k-ϵ models. The k-ω model is utilized near the walls whereas the k-ϵ model is useful as it approaches the free-stream. The SST models are typically less sensitive to the free stream conditions than the typical k-ω models, which prevents the buildup of excessive turbulent kinetic energy around stagnation points. The transport equations[10] for the turbulent kinetic energy k, and the specific dissipation rate ω, are modelled as:

$$\frac{\partial}{\partial t}(\rho k) + \frac{\partial}{\partial x_i}(\rho k u_i) = \frac{\partial}{\partial x_j}\left(\Gamma_k \frac{\partial_k}{\partial x_j}\right) + G_k - Y_k + S_k \quad (5)$$

$$\frac{\partial}{\partial t}(\rho \omega) + \frac{\partial}{\partial x_i}(\rho \omega u_i) = \frac{\partial}{\partial x_j}\left(\Gamma_\omega \frac{\partial_\omega}{\partial x_j}\right) + G_\omega - Y_\omega + D_\omega + S_\omega \quad (6)$$

Where, G_k denotes the development of turbulent kinetic energy due to mean velocity gradients, G_ω the generation of ω, Γ_ω and Γ_k the effective diffusivity of k and ω, respectively. Y_k and Y_ω reflect the turbulence- induced dissipation of k and ω. D_ω denotes the cross-diffusion. S_k and S_ω are source terms.

2.4 Geometry

To analyze the hemodynamic flow across the carotid artery bifurcation, a two-dimensional geometry of the structure was created while maintaining its key characteristics.

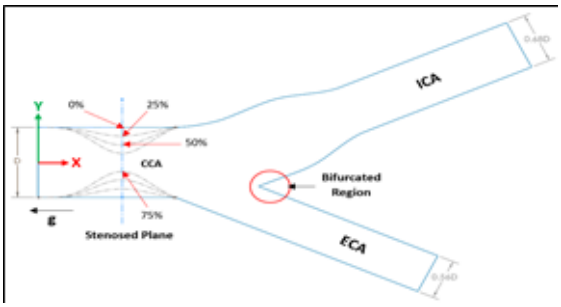

Figure 1. Carotid artery bifurcation model with proportion of stenosed areas.

Similar to previous work, the dimensions were carefully chosen to closely replicate the physiological conditions of blood flow in these arteries[11]. The geometric parameters were utilized to create the final 2D stenotic models (Figure 1) using the *SOLIDWORKS* software.

The flow geometry is sectioned into: the stenosed CCA (inlet), ICA (outlet), and ECA (outlet), with lengths of 1D, 0.68D and 0.56D respectively. Different stages of stenosis are developed in the CCA region. The radius of the normal artery at inlet is $R_o = D/2$ (D=6.30 mm). Radius of the dilated zone in each stage of stenosis was calculated based on a specific relation[12]:

$$R = R_0\left[1 - \frac{1}{4}\left(\frac{R_0 - R_{min}}{R_0}\right)\left(1 - \cos\left(\frac{\pi x}{D}\right)\right)^2\right] \quad (7)$$

Where, R_{min} is the minimum radius at the stenosis center. This study includes four stages of stenosis for the numerical solutions being 0% (no stenosis/healthy), 25% (low), 50% (mild) and 75% (severe). The healthy state was considered as a baseline to compare the effects of successive phases in the stenosed and bifurcated regions.

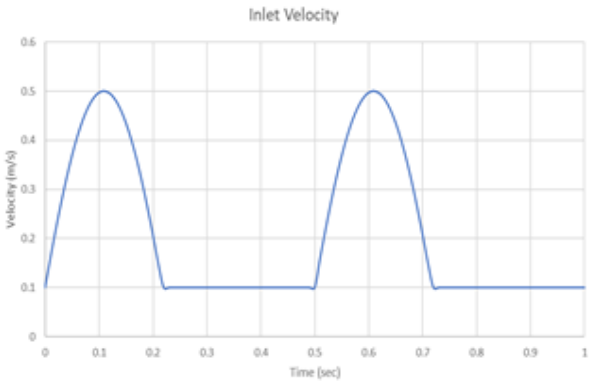

Figure 2. Inlet velocity (m/s) flow with time (s).

2.5 Boundary Conditions

Incorporating suitable boundary conditions is essential for a plausible and precise simulation. The presence of gravity (g) at 9.81 m/s^2 and the artery walls being rigid with no slip condition has been considered. Velocity at the inlet is programmed to be a time-varying periodic profile in a sinusoidal pattern.

A combination of two systolic phases has been considered constituting the pulsatile profile as shown in Figure 2. During the systolic phase, the sine wave has a peak velocity of 0.5 m/s and a minimum velocity of 0.1 m/s with each period lasting 0.5 seconds[13]. The analysis took into consideration two continuous cardiac cycles.

The boundary conditions are conventional by Ansys Fluent standards and methods. It is also to be noted that the reverse flow of fluid is prohibited at the outlets of the ECA and ICA. Initially, stress-free conditions with zero-gauge pressure are applied at the outlets.

2.6 Grid Independence Test

Numerical meshing and simulations for the study were carried out in Ansys Fluent (Ansys Academic Student 2022). Meshing in Ansys is structured with quadrilateral elements (Figure 4) along with some triangular elements created to maintain precision of the calculations in the fluid domain as well as to produce mesh in the stenotic section and bifurcation that is finer. Grid tests were carried out to ensure a mesh independent solution by modifying this mesh and carrying out computations repeatedly until there were no significant deviations. The maximum velocity was computed per meshed model, and the results can be visualized in Figure 3.

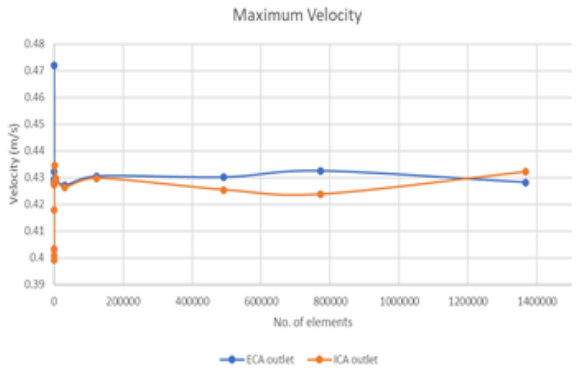

Figure 3. Maximum velocity (m/s) for range of mesh elements.

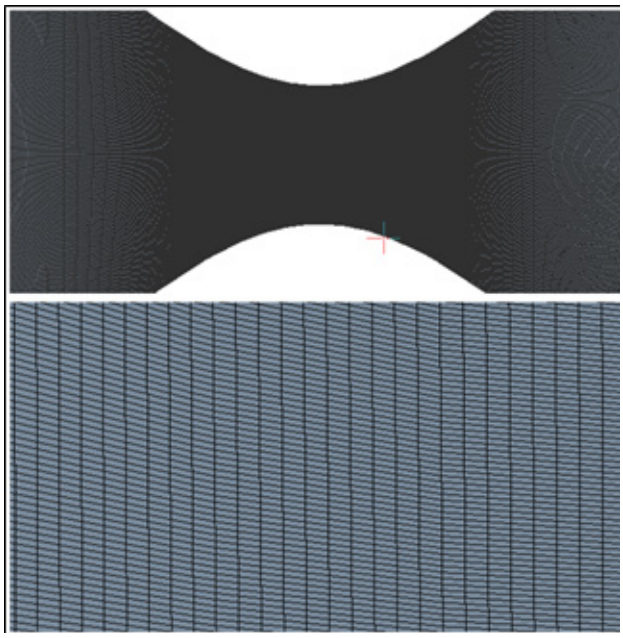

Figure 4. Quadrilateral mesh in stenotic area.

For results to be independent of the mesh, a mesh with more than 4,00,000 elements is advisable. The mesh size of 0.025 mm was used for all stages since the variations between the results were marginal, and 4,92,228 elements were created for zero percent stenosis condition.

2.7 Computational Details

To begin with, we solve the 2D unsteady Navier-Stokes equation in Fluent, which employs the finite volume discretization method, using the conservation equations in integral form. Following the conservation equations, the domain of solution was further divided into a finite number of continuous control-volumes. At different locations, the numerically solvable discrete system of algebraic equations was obtained as a function of space and time. The discretized equations were solved using an iterative approach because they were not linear. In this study, the governing equations were separated from one another and solved sequentially using the Semi Implicit Method for Pressure Linked Equations (SIMPLE) technique.

Additionally, Ansys Fluent by default maintains discrete scalar values at the central position of cells. Notwithstanding this, since parameters of the cell faces are unknown, they were treated as interpolating values based on the cell center values. An upwind method of

second order accuracy was used in this experiment. The cell-centered solution with respect to its centroid using Taylor's series yielded better accuracy at cell faces. In this analysis, 100-time steps were selected for two cardiac cycles with a step-size of 0.01s.

3.0 Results and Discussions

The model-based transient simulation results were analyzed to obtain velocity, flow pattern, pressure drops, and WSS distributions, all of which have a significant impact on the diagnosis of arterial disorders in medical settings.

Transient simulations for various stages of stenosis were conducted spanning from t = 0 to t = 0.5 s, followed by t = 0.5 s to t = 1 s, resulting in a heart rate of 120 beats/min[13].

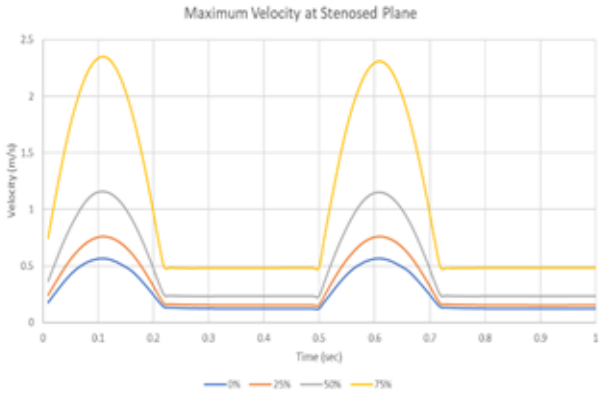

Figure 5. Maximum velocity (m/s) at stenosed plane for different stages with time (s).

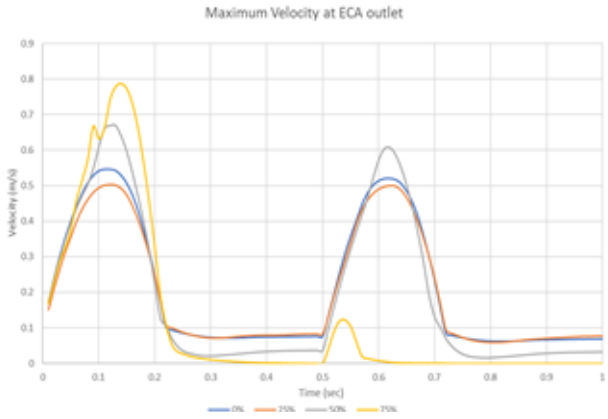

Figure 6. Maximum velocity (m/s) at ICA outlet for different stenosis stages with time (s).

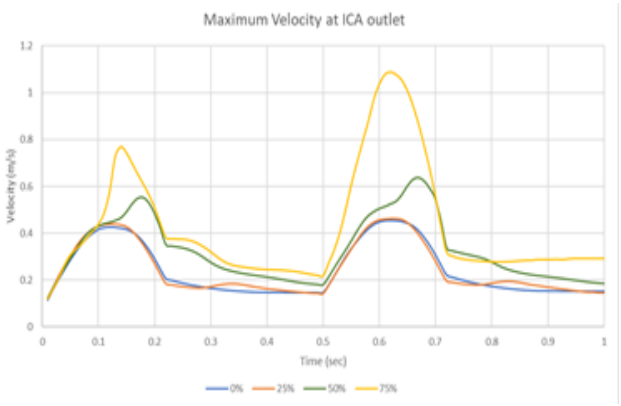

Figure 7. Maximum velocity (m/s) at ECA outlet for different stenosis stages with time (s).

3.1 Velocity

In order to effectively obtain the information that may be helpful for actual diagnostics, the peak velocities from the present simulations were compared at three different locations: the Stenotic Plane (SP), ICA outlet, and ECA outlet.

According to the simulation results, when the peak velocity at the CCA inlet is 0.5 m/s, the peak velocities were found to be 0.567 m/s in the no stenosis condition, 0.762 m/s in low stenosis, 1.160 m/s in mild stenosis, and 2.350 m/s in severe stenosis condition at SP over the two cardiac cycles, which is approximately a 414.46% increase in velocity from no stenosis to severe stenosis condition. The simulation results for all stages of stenosis are shown in the graphs (Figure 5 to 7).

In severe stenosis cases compared to healthy conditions, there has been a considerable rise in the velocities at all of the measured locations which is evident from the graphs. While there is a slight difference between low stenosis observations and healthy conditions, it has been shown that in case of severe stenosis, the mass flow rate at the ECA outflow is low as shown in Figure 15, which may result in a low peak velocity in the second cardiac cycle (Figure 7). Greater inconsistencies in outlet velocity (Figure 6 and 7) have been seen during both mild and severe cardiac cycles. The bifurcation geometry with larger flow separation in the fluid domain is the primary factor contributing to non-uniformity in velocity measurements at outlets with severe stenosed conditions.

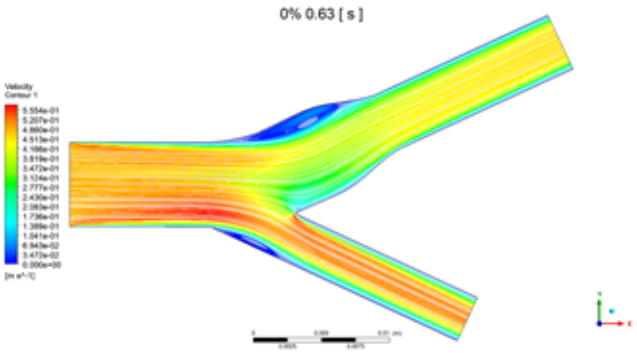

Figure 8. Velocity (m/s) contour and vortex formation in 0% stenosis at 0.63s.

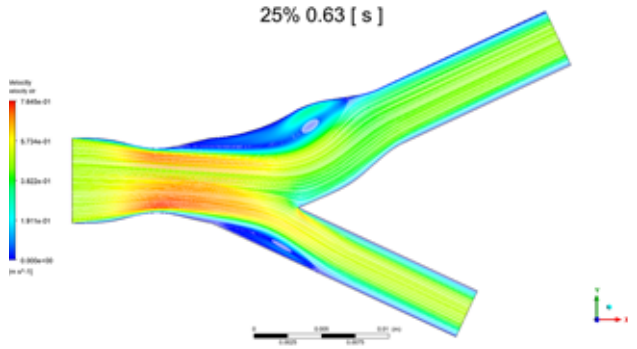

Figure 9. Velocity (m/s) contour and vortex formation in 25% stenosis at 0.63s.

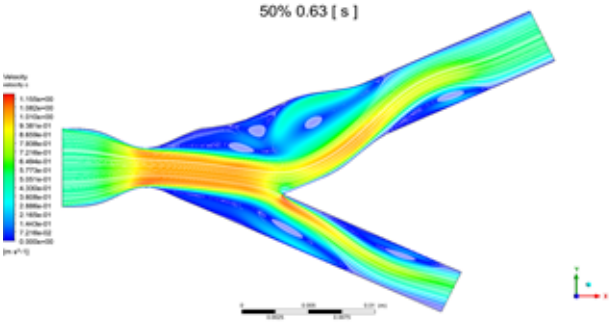

Figure 10. Velocity (m/s) contour and vortex formation in 50% stenosis at 0.63s.

3.2 Flow Separation

Previously, blood flow patterns had been thought to be distinct indications of susceptible plaque. When an artery becomes stenotic, the flow patterns can drastically shift. The figures (Figure 8 to 12) clearly indicate that the more severe the stenosis, the larger the separating vortex will become and this was considered for the

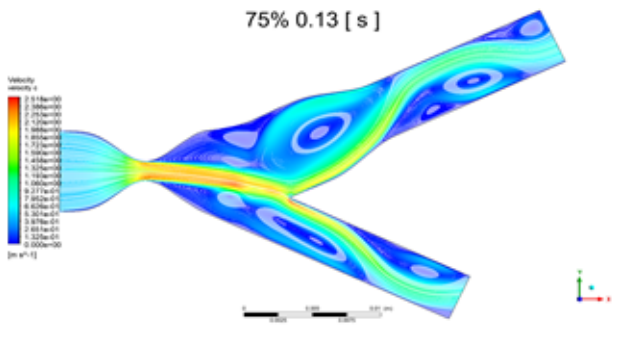

Figure 11. Velocity (m/s) contour and vortex formation in 75% stenosis at 0.13s.

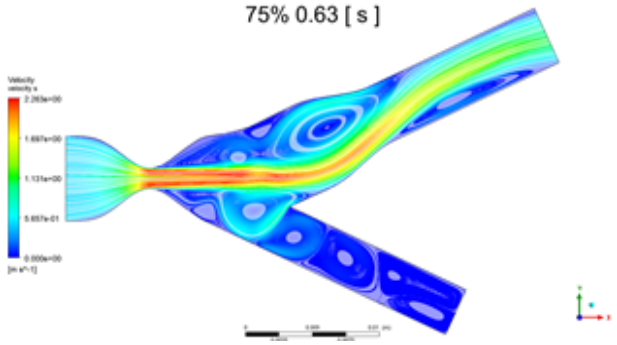

Figure 12. Velocity (m/s) contour and vortex formation in 75% stenosis at 0.63s.

cardiac cycles in case of healthy, low and mild stenosis conditions also. Whereas, for the case of severe stenosis conditions, significant variation was observed over both the systolic phases (Figure 11 and 12). This can be justified by observing the pattern of blood flow in the ICA and ECA. The presence of flow separation vortices in the post stenotic zones of severe stenosis, is a highly important phenomena[14], which is verified by the current CFD results.

3.3 Pressure Distribution

Although the flow rate decreases significantly at the ECA outlet (Figure 14), the pressure drop still increases with the increase of the percentage of stenosis. The effect of flow separation and vortex formation after the first cardiac cycle is demonstrated by the rapid fall in mass flow rate in mild and severe cases at the ECA outlet and an increase at the ICA outlet shown in Figure 13 during the second cardiac cycle. Figure 15 and 16 show that the pressure drop across the constriction is large during the systolic

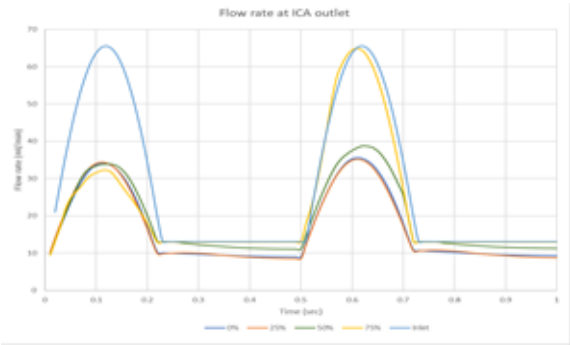

Figure 13. Flow rate (ml/min) at ICA outlet for different stenosis stages with time (s).

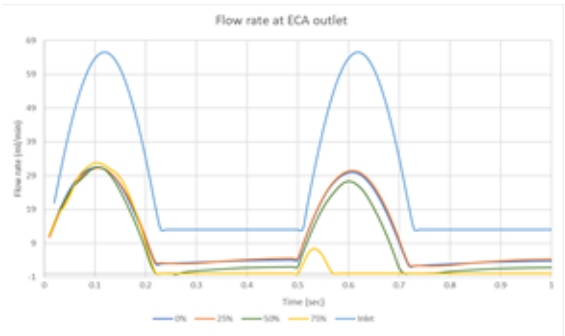

Figure 14. Flow rate (ml/min) at ECA outlet for different stenosis stages with time (s).

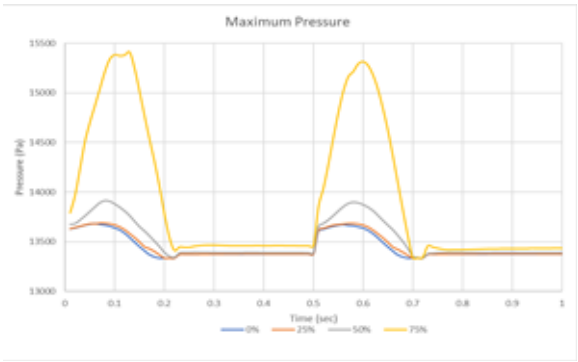

Figure 15. Maximum pressure (Pa) for different stenosis stages with time (s).

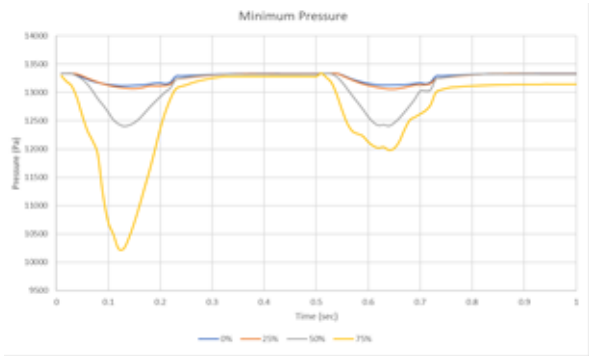

Figure 16. Minimum pressure (Pa) for different stenosis stages with time (s).

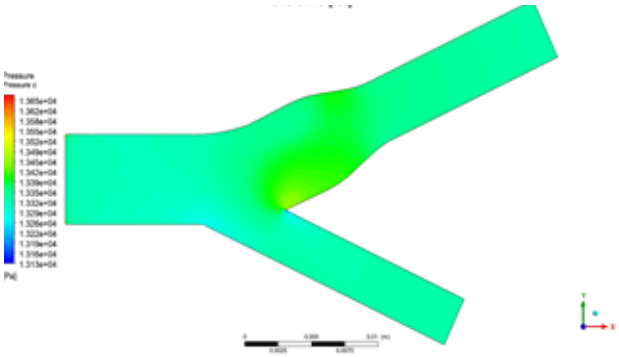

Figure 17. Pressure (Pa) contour in 0% stenosis at 0.13s.

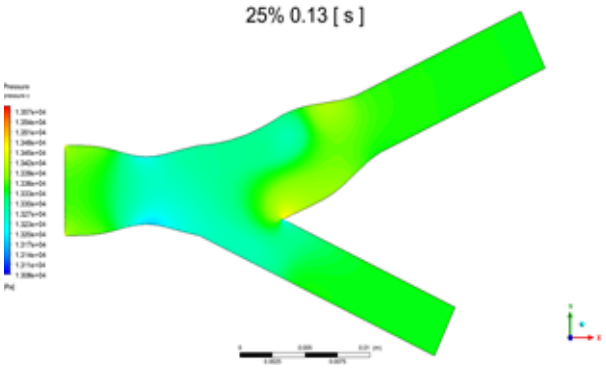

Figure 18. Pressure (Pa) contour in 25% stenosis at 0.13s.

phase in 50% and 75% stenosis, but minimal during the diastolic phase in 25% and 50% stenosis condition. As a result, for 75% stenosis, the pressure decrease across the stenosis is large throughout the cycle.

The above graphs show that as the degree of stenosis increases, the pressure differential throughout the stenotic zone worsens, with some impacts also in the bifurcation region, as shown in the pressure contours (Figure 17 to 20) with global legend values (Pressure in Pa). The upper limit difference exceeds 2000 Pa in severe stenosis cases and 500 Pa in mild stenosis cases. The lower drop was greater than 3000 Pa and 900 Pa in severe stenosis and mild stenosis respectively. The current CFD results confirm as the radius gets smaller, the pressure drop

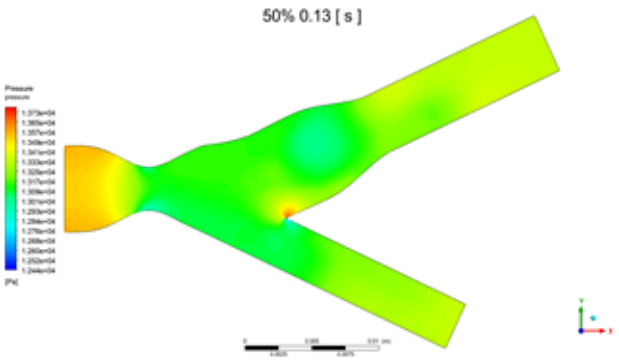

Figure 19. Pressure (Pa) contour in 50% stenosis at 0.13s.

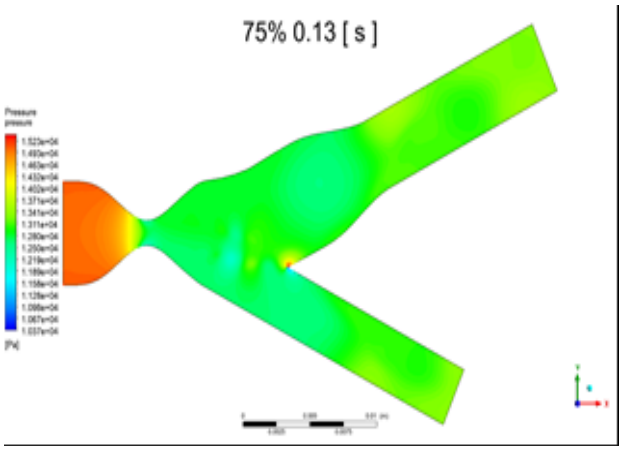

Figure 20. Pressure (Pa) contour in 75% stenosis at 0.13s.

eventually gets bigger[2] and also confirms that the blood flow is non-Newtonian and pulsatile.

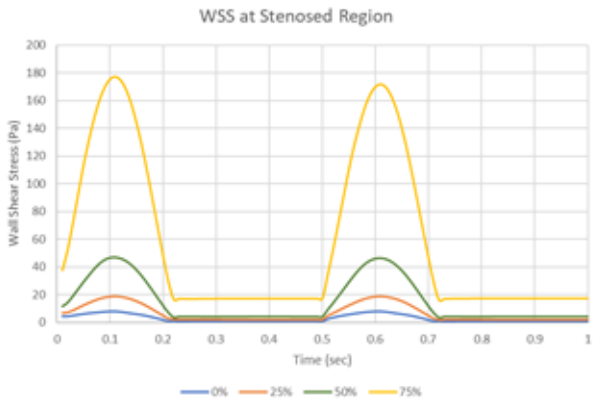

Figure 21. Maximum WSS (Pa) for different stenosis stages with time (s).

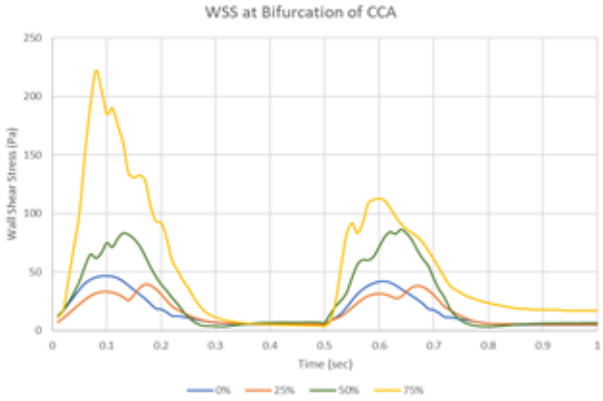

Figure 22. Maximum WSS (Pa) at bifurcation region for different stenosis stages with time (s).

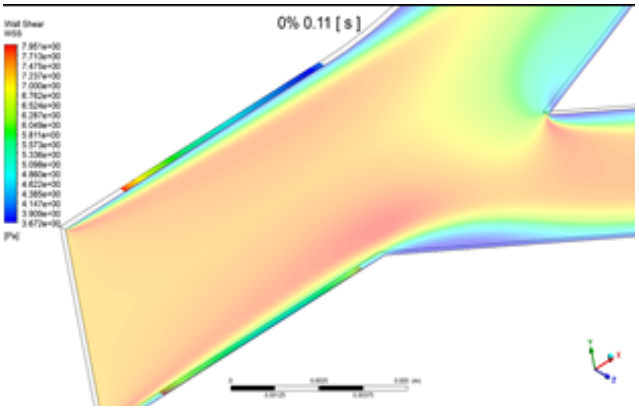

Figure 23. WSS (Pa) at stenosed region wall in 0% stage at 0.11s.

3.4 Wall Shear Stress

One of the most crucial hemodynamic parameters is the distribution of Wall Shear Stress (WSS), which has a substantial effect on the development of atherosclerosis. The distributions of maximum WSS for various stenosis severity levels are presented in the figures (Figure 23 to 26), along with a reference to the fluid domain in greater transparency. Additionally, it is clear that the maximal WSS across the severely stenotic neck rises with severity.

The graphs show the maximum WSS obtained in varying time with all stages of stenosis at the stenosed (Figure 21) and bifurcated (Figure 22) region. As the area reduces in the stenosed throat, the maximum WSS drastically increases and from the numerical simulation it has been observed that the maximum WSS value in the local stenotic region can go as high as 177.17 Pa in the

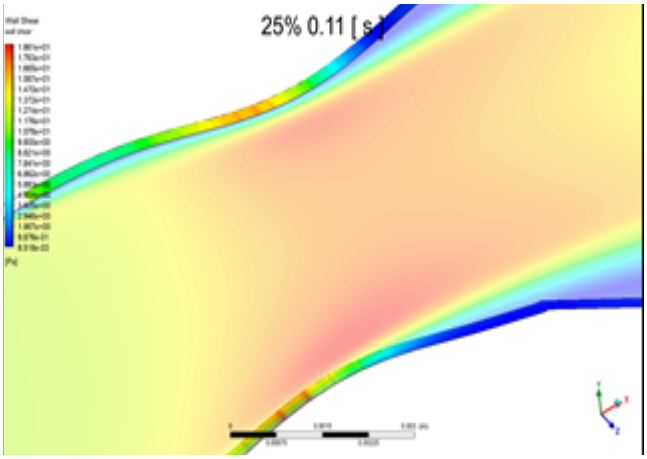

Figure 24. WSS (Pa) at stenosed region wall in 25% stage at 0.11s.

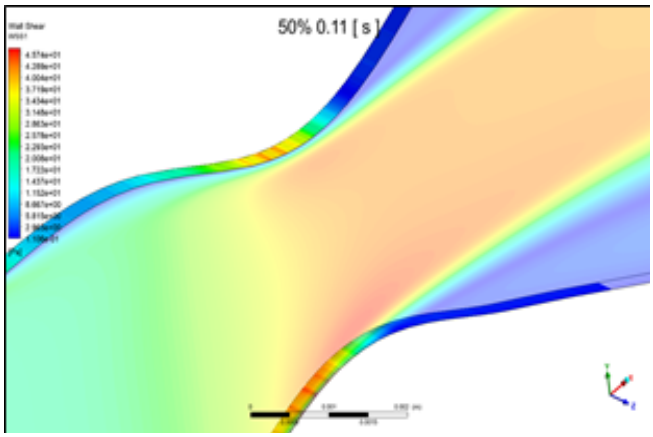

Figure 25. WSS (Pa) at stenosed region wall in 50% stage at 0.11s.

severe stage and 47.17 Pa and 18.80 Pa in the mild and low stenosis conditions respectively. On comparison of the stenotic data to a healthy region, the maximum WSS obtained is 7.97 Pa in the same region. From Figure 21, it is definite that the values are consistent for all stages in both the cardiac cycles. This is significant because it has been claimed that variations in WSS or disrupted flow promote increased endothelial cell turnover and artery wall intimal thickening. Increasing the WSS can result in embolism, which can lead to vascular blockage. The highest shear stress occurs in the stenosis's narrowest cross-section. The abrupt constriction of the stenosed lumen causes flow profile disruptions such as increased local WSS at the artery stenosis, the creation of post-stenotic vortices, and the establishment of a stagnation

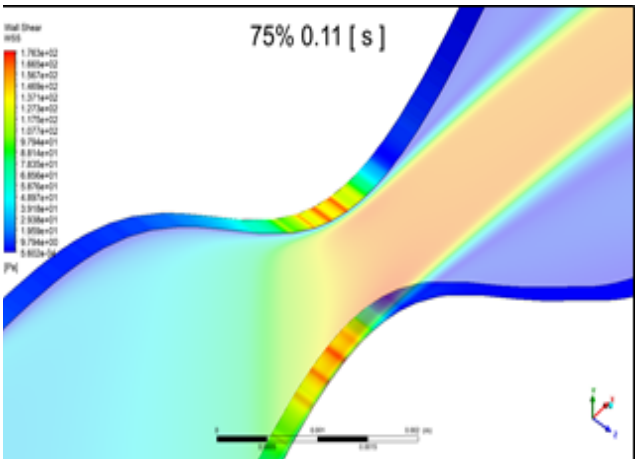

Figure 26. WSS (Pa) at stenosed region wall in 75% stage at 0.11s.

point. Both strong shear on the wall and stationary flow have been recognized as favorable circumstances for plaque formation via intrinsically distinct routes[14].

Since the flow is extensively redirected towards the ICA in advanced stages of stenosis, WSS at the bifurcation area shows that it rises with increase in plaque in the artery. Though there was a minimal difference in the maximum WSS values at the bifurcated region between healthy and low stage having the peak values 46.81 Pa and 39.43 Pa respectively. There was a significant increase in the values of higher degrees of stenosis. Over both the cardiac cycles, healthy, low and mild stages showed similar maximum WSS values with 46.81 Pa, 39.43 Pa and 86.66 Pa but there was an inconsistency in the severe stage with 222.30 Pa in the first cycle and 112.95 Pa in the second. This was mainly due to difference in flow pattern and mass flow over both the cycles which was also observed in flow separation and mass flow rate study. The figures (Figure 23 to 26) depict the variations in WSS with global legend values in the stenosed area as the degree of stenosis increases.

4.0 Conclusions

Although CFD has been extensively used to examine arterial stenosis, earlier research focused on the blood flows using particular patient-specific artery models, which may have limited coverage. Several studies have only used the Newtonian constitutive model for CFD modelling, which is insufficient to accurately represent

blood rheology. As a result, the current study is important because it depicts a traditional bifurcation of the CCA model at various degrees of arterial stenosis while accounting for pulsatile blood flow in the non-Newtonian Carreau model with SST k-ω turbulence model. Additionally, CFD studies demonstrate how a specific vascular contraction point negatively impacts blood flow, raising WSS at the stenosis site. Post the constriction, a rise in blood velocity and vortex formations lead to vessel occlusion and strokes.

The findings show that severe stenosis might lead to a significant pressure drop across the stenosed throat in CCA, ranging from 10,235 Pa to 15,410 Pa in the stenosed region compared to 13,117 Pa to 13,683 Pa in the healthy artery. The results of the simulation show that at peak systole, the maximum velocity at the throat in severe stenosis is 2.350 m/s, against a value of 0.567 m/s in the healthy artery. Maximum WSS shows a peak of about 177.17 Pa attained at the neck of severe stenosis, which is higher than the 7.97 Pa measured in a healthy artery and high enough to harm the endothelial cells. Furthermore, there is scope for more research in complex physiological flows and testing the accuracy of existing numerical results with actual patient data as well as alternative turbulence models to combine with our study which can then be used to design better treatment choices including the designing of stents from different materials based on degree of stenosis and using of Ag-Au (Silver-Gold) nanoparticles to improve the hemodynamics of the patient[15].

5.0 Acknowledgement

We acknowledge and appreciate the efforts of each author in carrying out the study and dissecting the findings. There is no disagreement between the writers' opinions.

6.0 References

1. Cheng Tu, Michel Deville. Pulsatile flow of non-Newtonian fluids through arterial stenoses. J. Biomech. 1996 July; 29(7):899-908. https://doi.org/10.1016/0021-9290(95)00151-4
2. Long Q, Xua XY, Ramnarineb KV, Hoskinsb P. Numerical investigation of physiologically realistic pulsatile flow through arterial stenosis. J Biomech. 2001 Oct.; 34(10):1229-42. https://doi.org/10.1016/S0021-9290(01)00100-2
3. Chan WY, Ding Y, Tu JY. Modeling of non-Newtonian blood flow through a stenosed artery incorporating fluid-structure interaction. ANZIAM J. 2005 Nov. 21; 47:C507-23 https://doi.org/10.21914/anziamj.v47i0.1059
4. Sankar DS, AhmadIzaniMd Ismail. Two-Fluid Mathematical Models for Blood Flow in Stenosed Arteries: A Comparative Study. Boundary Value Problems. 2009 Feb. 10; Article number:568657 https://doi.org/10.1155/2009/568657
5. Moreno C, Bhaganagar K. Modeling of Stenotic Coronary Artery and Implications of Plaque Morphology on Blood Flow. Hindawi Publishing Corporation Modelling and Simulation in Engineering. 2013 Nov. 12; Article ID: 390213. https://doi.org/10.1155/2013/390213
6. Mahalingam A, Gawandalkar UU, Kini G, Buradi A, Araki T, Ikeda N, Nicolaides A, Laird JR, Saba L, Suri JS. Numerical analysis of the effect of turbulence transition on the hemodynamic parameters in human coronary arteries. Cardiovascular Diagnosis and Therapy. 2016 Jun; 6(3):208-20. https://doi.org/10.21037/cdt.2016.03.08
7. Eshtehardi P, Brown AJ, Bhargava A, Costopoulos C, Hung OY, Corban MT, Hosseini H, Gogas Bill D, Giddens DP, Samady H. High wall shear stress and high-risk plaque: an emerging concept. Int J Cardiovasc Imaging. 2016 July; 33(7):1089-99. https://doi.org/10.1007/s10554-016-1055-1
8. Moradicheghamahi J, Sadeghiseraji J, Jahangiri M. Numerical solution of the Pulsatile, non-Newtonian and turbulent blood flow in a patient specific elastic carotid artery. Int J Mech Sci. 2019 January; 150:393-403. https://doi.org/10.1016/j.ijmecsci.2018.10.046
9. Nagargoje MS, Mishra DK, Gupta R. Pulsatile flow dynamics in symmetric and asymmetric bifurcating vessels. Physics of Fluids. 2021 July 1; 33(7):071904. https://doi.org/10.1063/5.0056414
10. Carvalho V, Rodrigues N, Lima RA, Teixeira S. Modeling Blood Pulsatile Turbulent Flow in Stenotic Coronary Arteries. Int J Biol Biomed. 2020 Nov.; 14(22):160-8. https://doi.org/10.46300/91011.2020.14.22
11. Perktold K, Resch M, Peter RO. Three-Dimensional Numerical Analysis of Pulsatile Flow and Wall Shear Stress in the Carotid Artery Bifurcation. J. Biomechanics. 1991; 24(6):409-20. https://doi.org/10.1016/0021-9290(91)90029-m
12. Husain I, Labropulu F, Langdon C, Schwark J. A comparison of Newtonian and non-Newtonian models for

pulsatile blood flow simulations. J Mech Behav Mater. 2013; 21(5-6):147-53. https://doi.org/10.1515/jmbm-2013-0001

13. Sinnott M, Cleary PW, Prakash M. An investigation of pulsatile blood flow in a bifurcation artery using a grid-free method. Fifth International Conference on CFD in the Process Industries (Australia). 2006 Dece; pp. 13-5.
14. Filardi V. Carotid Artery Stenosis near a Bifurcation Investigated by Fluid Dynamic Analyses. Neuroradiol J. 2013 Aug. 27; 26(4):439-53. https://doi.org/10.1177/197140091302600409
15. Tripathi J, Vasu B, Anwar Bég O. Computational simulations of hybrid mediated nano-hemodynamics (Ag-Au/Blood) through an irregular symmetric stenosis. Comp Biol Med. 2021 Mar.; 130:104213. https://doi.org/10.1016/j.compbiomed.2021.104213